Large neutral fractions in collisions of Li^+ with a highly oriented pyrolytic graphite surface: Resonant and Auger mechanisms

F. Bonetto,[1] M. A. Romero,[1] Evelina A. García,[1] R. A. Vidal,[1] J. Ferrón,[1,2] and E. C. Goldberg[1,2]

[1]*Instituto de Desarrollo Tecnológico para la Industria Química (INTEC) and Consejo Nacional de Investigaciones Científicas y Técnicas (CONICET), Güemes 3450, CC 91, 3000 Santa Fe, Argentina*

[2]*Departamento de Materiales, Facultad de Ingeniería Química, Universidad Nacional del Litoral, Santiago del Estero 2829, 3000 Santa Fe, Argentina*

(Received 10 April 2008; revised manuscript received 25 July 2008; published 18 August 2008)

We report measurements of neutral atom fractions for Li^+ scattered by a highly oriented pyrolytic graphite surface as a function of the incident ion energy and exit angle. We found an unexpected large neutralization probability that increases with both energy and exit angle. Based on a dynamical quantum calculation of the scattering process that accounts for the extended features of the surface and the localized nature of the atom-atom interactions, we propose that the resonant neutralization to the Li ground state is a relevant mechanism in this collision. However, to understand the whole process including the angular dependence, and taking into account the Li energy-level variations, we conclude that other mechanisms such as Auger neutralization to the ground state and resonant neutralization to excited states should also be considered.

DOI: 10.1103/PhysRevB.78.075422 PACS number(s): 79.20.Rf, 68.49.Sf, 71.27.+a

I. INTRODUCTION

Charge transfer between an atom (ion) and a surface is a very complex phenomenon whose implications extend over a large number of different fields, going from chemical reactions, as in catalysis for instance, to electron emission and surface characterization.[1,2] Since electron emission is usually coupled to the neutralization of the incoming ion, the understanding of the charge-transfer mechanisms in both processes, electron emission and ion neutralization, is a key fact in surface science characterization. The interaction between slow ions and a surface is a basic phenomenon that has received a lot of attention for more than a century. However, and despite the enormous amount of work devoted to the subject, new exciting experiments and theoretical models keep promoting a lot of debate.[1–3]

Auger neutralization[4] (AN) is, when possible, probably the most efficient neutralization mechanism in ion-surface collisions. In this process, the Coulomb repulsion between two electrons in the solid promotes the neutralization of the incoming ion through a tunneling effect of one of the electrons and the energy promotion of the other one. If the incoming hole energy is larger than twice the surface work function, electron emission can be observed. The other relevant mechanism for ion neutralization is resonant neutralization (RN). Here, the neutralization occurs when one-electron tunnels from the conduction band of the solid to a projectile energy level that lies within the valence band, i.e., no energy transfer is involved in RN. After that, the energy release may involve electron emission, for instance through a Coster-Kronig transition (AN involving electrons and holes within the valence band). Other but less probable mechanisms that could be involved in the electron production are Auger de-excitation (AD), where the interacting electrons belong one to the solid and the other to the incident projectile, and plasmon de-excitation.[2]

High ion yields and large elastic-scattering cross sections are some of the desirable conditions for good quality in low energy ion scattering (LEIS) experiments. To avoid the projectile neutralization during its collision with the surface, the projectile energy level should lie close to the surface work function. As Li^+ fulfils both requirements with many surfaces it appears to be a good projectile choice. Neither AN nor RN is expected in this case. However, this simplistic picture of the charge-exchange process usually fails. Yarmoff *et al.* showed that the resonant charge transfer (RCT) plays a role in the neutralization of Li^+ ions with several surfaces in Ref. 5 and references therein, and that neutralization of alkali ions is sensitive to the electronic states close to the surface Fermi level. Kimmel and co-workers[6,7] studied the neutralization process of low energy (5–1600 eV) alkali projectiles on Cu(001) and showed the sensitivity of the RCT process to the atomic resonances near the surface. Recently, it was showed that for the Li^+/Al system the electron emission may be understood as purely kinetic.[8] On the other hand, German *et al.*[3] proposed, for the same system, the promotion of the Li $1s$ level and the formation of $(\mathrm{Li}\ 1s^1 2s^2)^*$, followed by AD as a mechanism for secondary electron emission.

Large neutral fractions were reported in low energy Li/Cu(001) collisions.[6,7] In this case the experiments were performed by using low energy ions (from 5 to 1600 eV) and a scattering geometry where the incident and exit angles are equal to 45°. The neutral fraction was found to decrease monotonically as the perpendicular velocity increases (perpendicular energy values between 4 and 300 eV). Marston *et al.*[7] presented an interesting theoretical attempt to treat many-body correlations within an Anderson-Newns description. The authors used a systematic $1/N$ expansion to take into account the spin degeneracy and went further by including excited atomic states and affinity levels in the calculation. Nevertheless, when compared with experiments, the neutralization probabilities calculated using this formalism gave worse results than those calculated with the noninteracting (spinless) one. The authors mentioned that one reason for the difference between both models is the lack of the interatomic correlations in their calculation of neutralization

to the Li ground state. Finally, they concluded that in the many-body calculation it is very important to include the role of the spin together with all the possible channels: neutral, excited, and negative atom states.

Very recently, an unexpectedly large and face dependent neutralization probability has been found for Li^+ impinging on the Cu(111) and Cu(100) surfaces and on the (111) surfaces of some noble metals (Ag and Au).[9–11] These experimental results were obtained for an exit angle of 90° and show a general trend of neutral fractions increasing for both high and low incoming energies, and also marked differences between Cu(001) and Cu(111) surfaces that cannot be described satisfactorily by using the jellium model. The authors suggest that their high neutralization fractions on the (111) surfaces could be explained in terms of dynamical nonresonant electron transfer involving the surface states.

In this work we present measurements of the neutralization probability of Li^+ impinging on highly oriented pyrolytic graphite (HOPG) for different energies and incident angles. Comparison of the experimental results with time-dependent quantum mechanical calculations leads us to suggest that resonant and Auger neutralization mechanisms may be actually present in the Li^+/HOPG collision.

II. EXPERIMENTAL SETUP

The experiments were performed in a LEIS system that consists of an UHV chamber (base pressure in the 10^{-9} mbar range), a mass analyzed ion gun, and a time-of-flight (TOF) spectrometer. The Li^+ ions were produced in a discharge source (Colutron) from a heated quartz tube filled with LiCl and were mass analyzed using a Wien filter. For LEIS-TOF measurements the ion beam is rapidly swept by applying a square-wave voltage to a pair of deflection plates located before a rectangular slit to produce a pulsed ion beam. The HOPG sample is then bombarded by this pulsed ion beam. Ions and neutrals scattered off the graphite surface were detected by time-of-flight methods.[12,13] The scattering angle was fixed at 45° and the incoming and exit angles, measured with respect to the surface plane, were varied between 10° and 35°. To separate the ions from the neutrals, after scattering from the graphite surface, we use a pair of deflection plates placed at the flight tube entrance. Finally, the scattered particles were detected by a channeltron electron multiplier (CEM) placed at the end of the flight tube (144 cm flight length). The trigger output of the deflection plates pulse generator is used as the start pulse for a multiple-stop time spectrometer (Microchannel Scaler-MCS). Every particle reaching the detector after being scattered by the sample generates a pulse that is accumulated in a particular time channel of the MCS. After a certain acquisition time the MCS yields a histogram of the distribution of particle flight times (TOF spectrum). The usual pulse repetition rate was 3 kHz.

The HOPG sample was mounted on a manipulator that allows the changing of the incident (α) and exit (β) angles. The HOPG sample was cleaved in air, just before installing it in the UHV chamber, and cleaned in UHV by annealing at 1000 °C (1 min) by direct electron bombardment of the rear side of the sample holder.

III. THEORY

We performed a dynamical quantum calculation based on an Anderson-Newns description of the scattering process that accounts for the extended features of the surface and the localized nature of the atom-atom interactions. In the past, Marston *et al.*[7] applied a many-body theory of charge exchange to understand the neutralization of alkali ions scattered off a Cu(001) surface. An important difference between our calculation and that of Marston *et al.* rests in the model interaction used to calculate the atom energy levels and coupling terms. In our model the properties of the interacting atoms and a realistic band structure of the surface are incorporated. The present theoretical model, within a spinless approximation to the Anderson-like interaction Hamiltonian, has been already satisfactorily employed to describe the resonant ion neutralization in several collision systems.[14] In this work the infinite correlation (U) approximation instead of the spinless one in order to consider the spin statistical effects in the charge-exchange process is used.[15] The infinite U approximation used is based on the equations of motion (EOM) method that was shown to provide more confident results than other methods based on the $1/N$ expansion, with N being the state degeneration.[15] A resonant mechanism of neutralization to the ground state is assumed, associated to the charge fluctuation $Li^+(1s^2) \leftrightarrow Li^0(1s^2 2s)$ and the total spin fluctuation $S=0 \leftrightarrow S=1/2$. The Li states involved in this charge (spin) fluctuation are

$$Li^+ \rightarrow |0\rangle; Li^0 \rightarrow |\sigma\rangle \quad \text{with} \quad \sigma = 1/2, -1/2,$$

and the Anderson Hamiltonian projected over this subspace has the form

$$H = \sum_{k,\sigma} \varepsilon_k \hat{n}_{k\sigma} + E_0 |0\rangle\langle 0| + \sum_{\sigma} E_{1/2} |\sigma\rangle\langle\sigma| + \sum_{k,\sigma} [V_{k,2s} \hat{c}^+_{k\sigma} |0\rangle\langle\sigma| + \text{H.c.}]. \tag{1}$$

Here k denotes the solid states with energy ε_k and occupation number operator $\hat{n}_{k\sigma} = \hat{c}^+_{k\sigma} \hat{c}_{k\sigma}$. The Li^+ $(1s^2)$ ion total energy is E_0 and $E_{1/2}$ is the total energy of the neutral atom ground state; $V_{k,2s}$ is the coupling between the surface k states and the Li atom $2s$ state.

The required Green functions

$$G_\sigma(t,t') = i\theta(t'-t)\langle\Phi_0|\{|\sigma\rangle\langle 0|_{t'}, |0\rangle\langle\sigma|_t\}|\Phi_0\rangle,$$

$$F_\sigma(t,t') = i\langle\Phi_0|[|\sigma\rangle\langle 0|_{t'}, |0\rangle\langle\sigma|_t]|\Phi_0\rangle, \tag{2}$$

are calculated by using the method of motion equations solved up to a second order in the coupling parameter[15] and taking into account the norm constraint

$$|0\rangle\langle 0| + \sum_{\sigma} |\sigma\rangle\langle\sigma| = 1.$$

The final differential equations obtained are

$$idG_\sigma(t,t')/dt = (1 - \langle|-\sigma\rangle\langle-\sigma|\rangle)_{t'}\delta(t-t') + \varepsilon_I G_\sigma(t,t') - i\sum_k V_{k,2s}(t)\langle|-\sigma\rangle\langle 0|\hat{c}_{k-\sigma}\rangle_{t'} e^{-i\varepsilon_k(t-t')} + \int_t^{t'} d\tau \Sigma_\sigma^A(t,\tau)G_\sigma(\tau,t'), \quad (3)$$

$$idF_\sigma(t,t')/dt = \varepsilon_I F_\sigma(t,t') - i\sum_k (2\langle n_{k-\sigma}\rangle - 1)V_{k,2s}(t) \times \langle|-\sigma\rangle\langle 0|\hat{c}_{k-\sigma}\rangle_{t'} e^{-i\varepsilon_k(t-t')} + \int_{t_0}^{t} d\tau \Sigma_\sigma^R(t,\tau)F_\sigma(\tau,t') + \int_{t_0}^{t'} d\tau \Omega_\sigma(t,\tau)G_\sigma(\tau,t'), \quad (4)$$

where $\varepsilon_I = E_{1/2} - E_0$ and

$$\Sigma_\sigma^A(t,\tau) = i\Theta(\tau - t)\sum_k V_{k,2s}^*(t)V_{k,2s}(\tau)(1 + \langle n_{k-\sigma}\rangle)e^{i\varepsilon_k(\tau-t)} = \Sigma_\sigma^{R*}(\tau,t),$$

$$\Omega_\sigma(t,\tau) = i\sum_k V_{k,2s}^*(t)V_{k,2s}(\tau)(2\langle n_{k\sigma}\rangle - 1)(1 + \langle n_{k-\sigma}\rangle)e^{i\varepsilon_k(\tau-t)},$$

$$\langle|\sigma\rangle\langle 0|\hat{c}_{k\sigma}\rangle_t = (-1/2)\int_{t_0}^{t} d\tau V_{k,2s}(\tau)e^{i\varepsilon_k(\tau-t)}[F_\sigma(\tau,t) - (2\langle n_{k\sigma}\rangle - 1)G_\sigma(\tau,t)].$$

The average occupation number of the band states $\langle n_{k\sigma}\rangle$ is given by the Fermi-Dirac function $\langle n_{k\sigma}\rangle = 1/[1 + e^{(\varepsilon_k-\mu)/k_BT}]$.

The boundary conditions for solving Eq. (4) are, in the case of $Li^+ \rightarrow Li^0$,

$$\langle|\sigma\rangle\langle\sigma|\rangle_{t_0} = \langle|-\sigma\rangle\langle-\sigma|\rangle_{t_0} = 0,$$

$$F_\sigma(t_0,t') = -G_\sigma(t_0,t'),$$

and in the case of $Li^0 \rightarrow Li^+$,

$$\langle|\sigma\rangle\langle\sigma|\rangle_{t_0} = \langle|-\sigma\rangle\langle-\sigma|\rangle_{t_0} = 1/2,$$

$$F_\sigma(t_0,t') = G_\sigma(t_0,t').$$

In this way we calculate $\langle\hat{n}_\sigma\rangle = |\sigma\rangle\langle\sigma|$ from its time derivative

$$d\langle\hat{n}_\sigma\rangle/dt = 2\ \mathrm{Im}\sum_k V_{k,2s}(t)\langle|\sigma\rangle\langle 0|\hat{c}_{k\sigma}\rangle_t,$$

and the neutral fraction as $P_{\mathrm{res}}^0 = 2\langle\hat{n}_\sigma\rangle$.

The atom energy and the hopping terms are obtained from a model Hamiltonian for the atom-surface adiabatic interaction based on the localized atom-atom interactions and also on the extended features of the surface states.[16] By using a linear combination of atomic orbitals $\phi_i(r-R_s)$ for the k states $\varphi_k = \Sigma_{i,R_s} c_{i,R_s}^k \phi_i(r-R_s)$ and performing a mean-field approximation of the many-body interaction terms, the following short-range contributions determine the atom energy-level variation with the distance to the surface (here the charge states of the atoms are frozen to their values for the noninteracting situation):

$$\tilde{\varepsilon}_I = \varepsilon_0 - \sum_{R_s} V_{2s,2s}^{Z_s,R_s} + \sum_{i,R_s}(2\tilde{J}_{2s,iR_s} - \tilde{J}_{2s,iR_s}^X)\langle n_i\rangle - \sum_{i,R_s} S_{2s,iR_s}V_{2s,iR_s}^{\mathrm{dim}} + \frac{1}{4}\sum_{i,R_s} S_{2s,iR_s}^2 \Delta E_{2s,iR_s}. \quad (5)$$

The $\varepsilon_0 - \Sigma_{R_s} V_{2s,2s}^{Z_s,R_s}$ term accounts for the one-electron contributions (kinetic energy and electron-nuclei interactions); $\tilde{J}_{2s,iR_s}, \tilde{J}_{2s,iR_s}^X$ are the direct and exchange Coulomb integrals calculated up to a second order expansion in the overlap S_{2s,iR_s} of the symmetric orthogonal basis set.[17] The $\Delta E_{2s,iR_s}$ corresponds to the difference between the projectile atom and surface-atom energy terms, $V_{2s,iR_s}^{\mathrm{dim}}$ is the off-diagonal term that also includes the two-electron contributions to the hopping within a mean-field approximation, and the superindex dim indicates that it is calculated within the orthogonal basis set for the corresponding dimmer $(0,R_s)$.[16] We use the atomic basis for C and Li atoms provided by Huzinaga *et al.*[18] including a p polarization function in the case of Li. The effect of the long-range interactions is introduced by considering the image potential defining the behavior for large normal distances (z) to the surface $(z > z_a)$:[14,16]

$$\varepsilon_I(R) = \begin{cases} \tilde{\varepsilon}_I(R) + V_{\mathrm{im}}(z_a) & \text{for } z \le z_a \\ \tilde{\varepsilon}_I(R) + V_{\mathrm{im}}(z) & \text{for } z > z_a, \end{cases} \quad (6)$$

where

$$V_{\mathrm{im}}(z) = \frac{1}{4(z - z_{\mathrm{im}})},$$

with $z_{\mathrm{im}} = 3.16$ a.u. for the HOPG surface and $z_a = 8$ a.u. is chosen to match the Hartree-Fock result $\tilde{\varepsilon}_I(R)$ with the correct behavior by the image potential contribution at large distances. With respect to the dynamical effects, we conserve the effect of the Galilean transformation only in the shift of the atomic level as seen from the surface.[14]

The energy levels calculated in this form correspond to $\varepsilon_I = E_{\mathrm{tot}}^{N+1} - E_{\mathrm{tot}}^N$, that is the difference between the total energies with $N+1$ and N electrons. For instance, the Li ionization energy is given by $\varepsilon_I = E_{\mathrm{tot}}^{N+1}(1s^2 2s) - E_{\mathrm{tot}}^N(1s^2) = E_{1/2} - E_0$. The coupling with the band states is calculated in the same way as: $V_{k,2s} = \Sigma_{i,R_s} c_{i,R_s}^k V_{iR_s,2s}^{\mathrm{dim}}$, where the coefficients c_{i,R_s}^k are related with the local density of states of the surface, $\rho_{i,j,R_s}(\varepsilon)$, through the expression $\rho_{i,j,R_s}(\varepsilon) = \Sigma_k c_{i,R_s}^{k*} c_{j,R_s}^k \delta(\varepsilon - \varepsilon_k)$.

IV. RESULTS

Figure 1 shows a typical TOF spectrum of total scattered (ions plus neutrals) and neutral particles for 3 keV incident Li ions and 20° exit angle. To estimate the neutral fraction at the elastic (surface) peak we integrated the spectra over a narrow TOF interval (5 channels=200 ns, $\Delta E \approx 140$ eV, striped region in the figure) centered at the elastic peak (position estimated using the elastic binary collision model).[13] The reason to use that part of the spectra close to the elastic

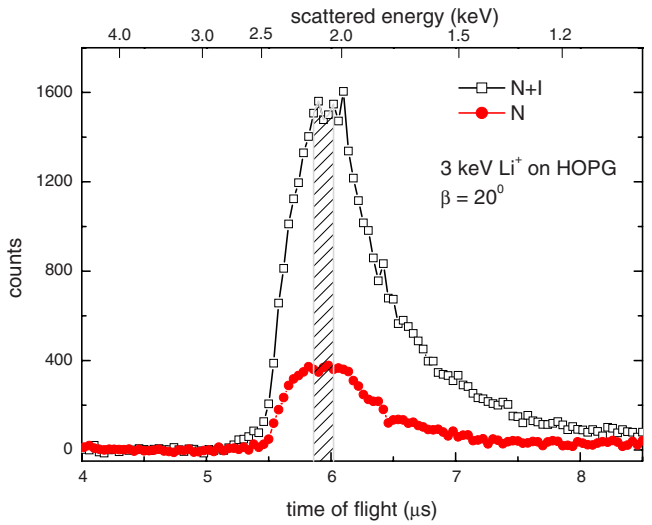

FIG. 1. (Color online) TOF-ISS spectra of total scattered ions plus neutral (open squares) and neutral (full circles) particles for $\alpha/\beta=25^0/20^0$ and for 3 keV Li^+ incoming energy. The striped area indicates the elastic peak width considered.

peak is to compare with theoretical results as they assume that the projectile scatters after a single binary collision with an atom at the surface.

In Fig. 2 we show the experimental neutral fractions for different incident energies and exit angles. An overall increase with incoming energy and exit angles can be observed in these curves. It is important to remark that the magnitudes of the measured neutral fractions are quite large for an ion whose ground-state level shifted by the image potential lies over the surface Fermi level.

In Fig. 3 we compare experimental neutral fractions with theoretical neutralization probabilities for 2 and 5 keV Li^+ on HOPG as a function of the exit angle.

The theoretical results from a spinless calculation are also included in Fig. 3 for comparison. It can be observed that the differences introduced by the spin fluctuations are more important for large outgoing normal velocities. This is due to the fact that the most remarkable electronic correlation effects take place at distances close to the surface, and the charge transfer defined in this distance region is maintained as faster the projectile leaves the surface.

Although a nice agreement among experiments and theory for large exit angles can be observed better in the case of including correlation effects, a departure for low exit angles is also evident. This result leads us to think that while the resonant neutralization to the ground state seems to be the main mechanism describing satisfactorily the experimental data for large exit angles, other mechanisms could be operating more efficiently for small values of normal velocities, i.e., at small exit angles.

V. DISCUSSION

The first goal of our theoretical model is to understand the physical reasons for the unexpectedly large neutralization probability for an ion whose ground-state level is so close to

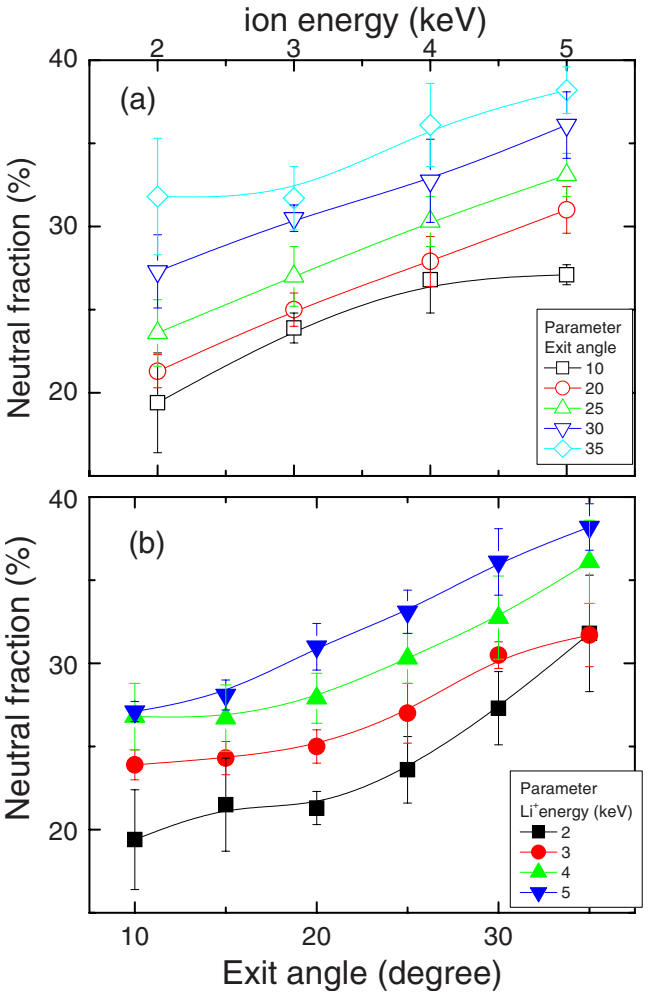

FIG. 2. (Color online) Experimental neutral fractions as (a) a function of incident energies (exit angle as a parameter) and (b) a function of exit angles (Li^+ incident energy as a parameter).

the substrate Fermi level. After that, we will focus our attention on the possible missing mechanisms that should be considered to account for the remaining differences between theory and experiments.

In Fig. 4 we depict the Li neutralization probability as a function of the perpendicular ion-surface distance (z) measured with respect to the corresponding turning point for an exit angle of 35° and 4 keV of incoming energy. The density of states (DOS) of HOPG (Ref. 19) and the evolution of the Li ionization level (solid line) along the ion trajectory are also depicted in this figure. Negative distance means incoming trajectory, and the asymmetry in the energy evolution comes from the different in-out trajectories. Two startling results are apparent in this figure: a large neutralization probability and a notable downshift of the ionization energy level close to the surface. Li ions are almost fully neutralized close to the surface, i.e., along the region where the ionization level reaches its minimum value.

After that, a lower asymptotic value (~30%) is reached as a consequence of the Li level variation and the coupling interactions. This effect naturally leads us to conclude that the downward shift of the Li ionization level is the main

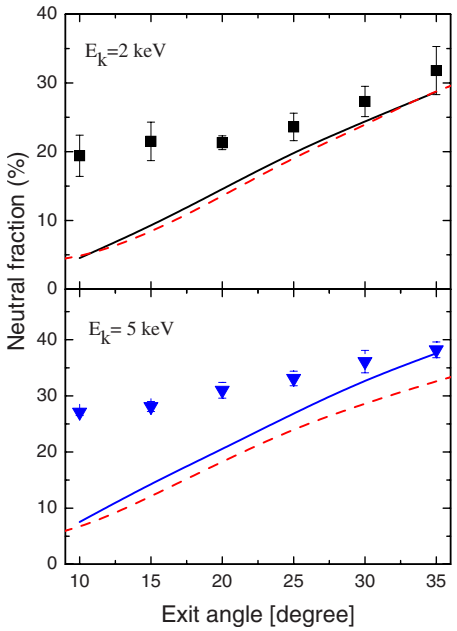

FIG. 3. (Color online) Li^+ neutralization probability as a function of exit angle. Experimental data: 2 keV (full squares) and 5 keV (full down triangles). Theoretical neutral fractions: dash line corresponds to the spin-less calculation and solid line to the calculation including correlation effects.

responsible of the neutralization caused by the resonant mechanism.

Thus, while a total neutralization of Li ions occurs close to the surface promoted by the pronounced downshift of the Li energy level, in our model the final occupation of the ground state is defined along the exit trajectory. In order to prove this, we calculated the neutral fraction for Li° bombardment. Figure 4 shows a remarkable similarity between

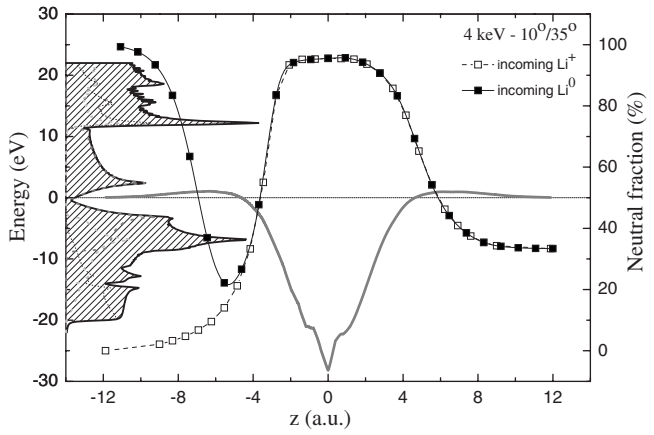

FIG. 4. Normal distance dependence of the calculated neutral fraction along the trajectory for the HOPG surface for $\alpha/\beta = 10^0/35^0$. Both curves correspond to 4 keV energy of incoming Li^+ (open squares) and Li^0 (full squares). Striped region corresponds to the HOPG total local DOS. The full gray line indicates the projectile ionization level energy as a function of z, referred to the surface Fermi level ($E_{\mathrm{Fermi}}=0$).

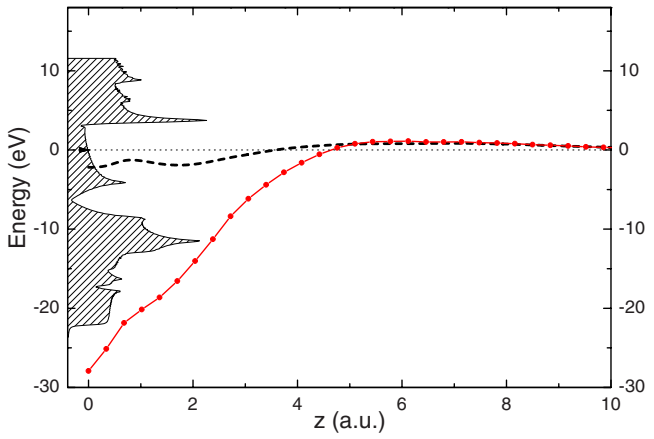

FIG. 5. (Color online) Evolution of the ionization level energy along the ion trajectory for $\alpha/\beta=35^0/10^0$ when the interaction with only one surface atom is considered (dashed line) and the interaction with many surface atoms is included (dot line). The striped area corresponds to the HOPG total local DOS.

Li^0 and Li^+ bombardment final neutral fractions, giving support to our assertion of a complete memory loss of the initial charge state on the incoming trajectory.

Since the Li energy-level downshift is the responsible of the main features of the charge-exchange process, its origin deserves a bit more of attention. The reason of the downshift of the ground-state energy level close to the surface is the interaction of the projectile with several atoms of the solid, originated in the extension of the Li atomic states, and the rather compact spatial distribution of graphite atoms. The energy-level variation given by Eq. (5) is finally determined from a detailed balance between attractive and repulsive terms such as $(-\Sigma_{R_s} V^{Z_s,R_s}_{2s,2s})$ and $(\Sigma_{i,R_s}(2\tilde{J}_{2s,iR_s} - \tilde{J}^X_{2s,iR_s})\langle n_i\rangle - \Sigma_{i,R_s} S_{2s,iR_s} V^{\mathrm{dim}}_{2s,iR_s})$, respectively.

In Fig. 5 we show the evolution of the Li ionization level (dot line) along the ion trajectory corresponding to an exit angle of 10° with respect to the surface plane, and the evolution of the same level when the interaction with only the scatterer surface atom at $R_s=(0,0,0)$ is considered (dashed line). The comparison between both evolutions shows the importance of the interaction with all the surface atoms that the projectile can "see" along its trajectory.

In what follows we will analyze the discrepancies between experimental and theoretical results. As we showed in Sec. IV, the resonant mechanism satisfactorily describes the experimental results for large exit angles, but it seems that another mechanism is operating for small normal velocities (exit angles). The variation of the Li ionization energy level shown in Fig. 5 lets us to conclude that for small ion-surface distances ($z<3$ a.u.), not only a resonant neutralization to the Li ground state is possible but also the Auger neutralization channel could be available. If this is the case, interference effects between Auger and resonant mechanisms along the interaction time evolution should be expected.[20] A correct estimation of the neutralization probabilities in this case would require a simultaneous quantum treatment of AN and RN, task that is beyond the scope of the present work. However, the AN contribution can be roughly estimated using a

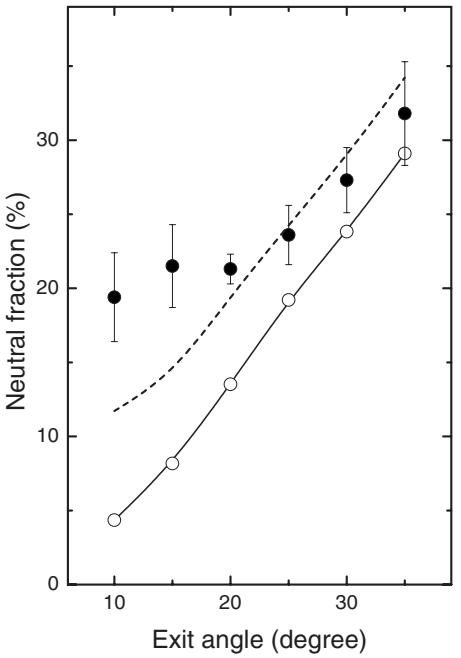

FIG. 6. Neutral fraction as a function of the exit angle for 2 keV Li^+ incoming energy. Full circles correspond to experimental results, open circles to theoretical results including only RN, and dashed line corresponds to the calculated neutral fraction when a rough estimation of the Auger neutralization contribution is added to RN (see text).

semiclassical calculation considering its probability as independent along the whole process. In this case the total ion fraction is calculated as

$$P^+ = P^+_{\text{Auger}} * P^+_{\text{Res}} = \exp[-v_0/(1/v^{\text{in}}_{\text{perp}} + 1/v^{\text{out}}_{\text{perp}})] * P^+_{\text{Res}}. \tag{7}$$

The best fit of the experimental data was obtained with $v_0 = 0.0015$ a.u. ($v^{\text{in/out}}_{\text{perp}}$ is the normal to the surface component of the ion velocity), and the neutralization probability ($1\text{-}P^+$) obtained by using Eq. (7) is depicted in Fig. 6 for 2 keV Li ions. The parameter v_0 characterizes the neutralization efficiency (it has to be with the integration of the Auger transition rate over the range of distances where the Auger process is operative). The value 0.0015 a.u. is 20 times smaller than the calculated one for the case of He/Al system,[21] denoting a less efficient Auger neutralization in the case of Li/HOPG.

There is even another possible neutralization channel that could explain the differences remaining between the theoretical and experimental results observed for small exit angles. Since excited neutral Li atoms have been observed via the optical $2p \rightarrow 2s$ transition in $Li^+/Cu(001)$ collisions,[7] the neutralization to the excited state $1s^2 2p$ should be taken into account. Within our model we can calculate, through an expression analogous to Eq. (5), the dependence of this excited-state energy with the distance to the surface. This result is shown in Fig. 7 where we can observe that resonant neutralization to the Li excited state $1s^2 2p$ is actually possible.

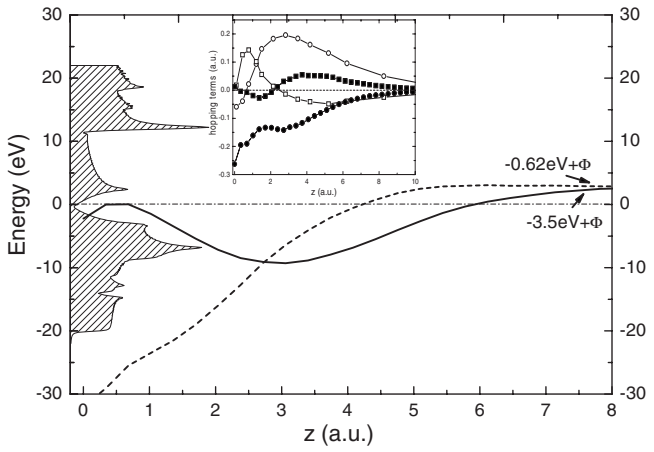

FIG. 7. Evolution of the affinity (dashed line) and excited Li-$1s^2 2p$ (solid line) level energies along the ion trajectory for $\alpha/\beta = 35^0/10^0$ (the corresponding asymptotic values are also indicated, $\Phi = 4.67$ eV is the HOPG work function). The striped area corresponds to the HOPG total local DOS. The following coupling terms are shown in the inset: Li($2s$)-C($2s$) (full circles); Li($2s$)-C($2p_z$) (full squares); Li($2p_z$)-C($2s$) (empty circles); and Li($2p_z$)-C($2p_z$) (empty squares).

According to the shift of the excited energy level one can expect strong many-body effects regulating the occupations of the ground and excited states along the dynamical evolution determined by the interplay of the two velocity components. The more extended character of the Li-$2p$ state is evident from the comparison of the hopping terms shown in the inset of Fig. 7; then, the occupation of the excited state is going to take place first along the incoming ion trajectory and interferences between the ground and excited-state populations could occur. In the case of He^+ scattered by a HOPG surface, it has been found that including the excited channel in the neutralization process makes more favorable the neutralization to the ground state due to electronic correlation effects.[23]

On the other hand, accordingly to the energy shift of the affinity level $\varepsilon_A = E^{N+1}_{\text{tot}}(1s^2 2s^2) - E^N_{\text{tot}}(1s^2 2s)$, which is also included in Fig. 7, the Li^- formation from Li^0 cannot be disregarded as an intermediary channel contributing to the final neutral fraction ($Li^0 \rightarrow Li^- \rightarrow Li^0$).

Other important point to take into account is the parallel velocity effect associated to the Galilean transformation and only partially considered in this work. Nevertheless, similar trends are found in the neutral fraction behavior observed in the case of Li/Cu(111) for the same range of velocities,[11] where parallel velocity effects are not expected because only outgoing trajectories normal to the surface are involved.

In summary, we have performed ion scattering spectroscopy (ISS)-TOF measurements of the neutralization probability for Li^+ on HOPG for various energies and exit angles. Comparison of the experimental results with calculations of the resonant neutralization probability to the ground state shows that the unexpected large neutral fractions can be explained in terms of the pronounced downshift of the energy

level caused by the short-range interactions between the projectile and the surface. In order to understand the whole energy and exit angular dependence, and taking into account the variation of the Li energy levels along the atom trajectory, other contributions arising from Auger and resonant mechanisms involving Li ground, first excited and negative states should be considered. The interferences between the different neutralization channels within an appropriate calculation that includes electronic correlation effects could change substantially the neutralization to the ground-state probability found in the case of neglecting the other less likely channels.[7,22,23]

ACKNOWLEDGMENTS

This work was supported by ANPCyT through Contracts No. PICT14730 and No. 14724, CONICET through Contract No. PIP 5277, and U.N.L. through CAI+D grants. We gratefully acknowledge C. González Pascual from Universidad Autónoma de Madrid for providing us the HOPG DOS.

[1] D. Valdés, J. M. Blanco, V. A. Esaulov, and R. C. Monreal, Phys. Rev. Lett. **97**, 047601 (2006).
[2] R. A. Baragiola and C. A. Dukes, Phys. Rev. Lett. **76**, 2547 (1996).
[3] K. A. H. German, C. B. Weare, and J. A. Yarmoff, Phys. Rev. Lett. **72**, 3899 (1994); Phys. Rev. B **50**, 14452 (1994).
[4] H. D. Hagstrum, Phys. Rev. **96**, 336 (1954).
[5] J. A. Yarmoff, Y. Yang, G. F. Liu, X. Chen, and Z. Sroubek, Vacuum **73**, 25 (2004).
[6] G. A. Kimmel and B. H. Cooper, Phys. Rev. B **48**, 12164 (1993).
[7] J. B. Marston, D. R. Andersson, E. R. Behringer, B. H. Cooper, C. A. DiRubio, G. A. Kimmel, and C. Richardson, Phys. Rev. B **48**, 7809 (1993).
[8] N. Bajales, S. Montoro, E. C. Goldberg, R. A. Baragiola, and J. Ferrón, Surf. Sci. Lett. **579**, 97 (2005).
[9] A. R. Canario, T. Kravchuk, and V. A. Esaulov, New J. Phys. **8**, 227 (2006).
[10] T. Kravchuk, Yu. Bandourine, A. Hoffman, and V. A. Esaulov, Surf. Sci. Lett. **600**, L265 (2006).
[11] M. Wiatrowski, N. Lavagnino, and V. A. Esaulov, Surf. Sci. Lett. **601**, L39 (2007).
[12] O. Grizzi, M. Shi, H. Bu, and J. W. Rabalais, Rev. Sci. Instrum. **61**, 740 (1990).
[13] H. H. Brongersma, M. Draxler, M. de Ridder, and P. Bauer, Surf. Sci. Rep. **62**, 63 (2007).
[14] M. C. Torralba, P. G. Bolcatto, and E. C. Goldberg, Phys. Rev. B **68**, 075406 (2003); Evelina A. García, C. González Pascual, P. G. Bolcatto, and E. C. Goldberg, Surf. Sci. **600**, 2195 (2006); F. Bonetto, M. Romero, Evelina A. García, R. Vidal, J. Ferrón, and E. C. Goldberg, Europhys. Lett. **80**, 53002 (2007).
[15] E. C. Goldberg, F. Flores, and R. C. Monreal, Phys. Rev. B **71**, 035112 (2005).
[16] P. G. Bolcatto, E. C. Goldberg, and M. C. G. Passeggi, Phys. Rev. B **58**, 5007 (1998).
[17] P. O. Lowdin, J. Chem. Phys. **18**, 365 (1950).
[18] S. Huzinaga, J. Chem. Phys. **42**, 1293 (1965); S. Huzinaga, J. Andzelm, M. Klobukowsky, E. Radzio-Andzelm, Y. Sakai, and H. Tatewaki, *Gaussian Basis Set for Molecular Calculation*, edited by S. Huzinaga (Elsevier, Amsterdam, 1984).
[19] O. F. Sankey and D. J. Niklewski, Phys. Rev. B **40**, 3979 (1989); A. A. Demkov, J. Ortega, O. F. Sankey, and M. P. Grumbach, *ibid.* **52**, 1618 (1995).
[20] Evelina A. García, N. P. Wang, R. C. Monreal, and E. C. Goldberg, Phys. Rev. B **67**, 205426 (2003).
[21] E. C. Goldberg, R. Monreal, F. Flores, H. H. Brongersma, and P. Bauer, Surf. Sci. **440**, L875 (1999).
[22] N. Bajales, J. Ferrón, and E. C. Goldberg, Phys. Rev. B **76**, 245431 (2007).
[23] N. B. Luna, F. J. Bonetto, R. A. Vidal, J. Ferrón, and E. C. Goldberg, J. Mol. Catal. A: Chem. **281**, 237 (2008).